Modelling of 1.55μm InGaAs/InP Multiquantum Well Lasers

M. T. Furtado
CPqD-TELEBRÁS, C P. 1579, Campinas, 13085, SP, Brasil

Received September 13, 1993

A theoretical model is presented foi multiquantum well (MQW) lasers emitting at 1.55μm based on an InGaAs/InP heterostructure as well as on an InGaAs/InGaAsP/InP separate confinement heterostructure (SCH). Both MQW structures are lattice matched to InP and the latter involves barrier and separate confinement layers of InGaAsP with composition corresponding to 1.3μm wavelength emission. We have analysed the influence of the number of QWs and the cavity length on tlie threshold current density and the external quantum efficiency, taking into account tlie intervalence band absorption losses in the QW layers. The threshold current density presents a minimum value as a function of the number of QWs, which decreases with increasing cavity length. The external quantum efficiency increases as both parameters decrease. However, tlic laser characteristics are improved with a smaller number of QWs in the SCH, due to the enhancement of tlie optical confinement factor. The results obtained are compared with theoretical predictions of a bulk active layer device emitting at the same wavelength.

I. Introduction

Multiquantum well (MQW) lasers have great technological interest, because the two-dimensional density of states in the active region offers several advantages over a bulk active layer. The gain peak increases more rapidly with tlic injected carrier density[1], and consequently MQW lasers exhibit a lower threshold current tlensity and a higher external quantum efficiency.

Much effort lias been devoted to tlie investigation of MQW lasers emitting in tlic attenuation minimum wavelength of optical fibres at 1.55μm because of useful applications in optical communications[2]. These devices usually involve a MQW structure which consists of InGaAs QW layers grown between InGaAsP barrier and confinement layers, and InP cladding layers, all grown oii an InP substrate. The main reasons for employing a MQW structure, are the low optical confinement factor of a thin single QW layer and the high optical losses in InGaAs due to intervalence band absorption. Although many results have been reported recently on tlie high performance of 1.55μm emitting MQW lasers[2-8], there is no report on a systematic study of the dependence of the device characteristics on tlie geometrical parameters of the laser cavity.

In tliis work, we have undertaken a systematical analysis of tlie thresliold current density and the external quantum efficiency of 1.55μm MQW lasers, in terms of the number of QWs in the active layer and the laser cavity length. In section II, we describe the calculation of tlie QW thickness dependence of the 1.55μm einission wavelength on tlie barrier layer composition. In tliis study, we have only considered lattice matched MQW heterostructures on InP substrates. Section III presents tlie model employed to determine the electro-optical characteristics of the MQW laser structure. In section IV, rve describe the results of a simple MQW structure comprising $In_{1-x}Ga_xAs$ (x=0.47) QW layers sandwiched between InP barrier and confining layers. The InGaAs/InP heterostructure is interesting because it has fewer growth parameters and involves the switching of only one V element in the epitaxial growth process, and therefore the QW interfaces can be more easily grown. Moreover, tlie advantages of the two dimensional density of states can be more easily compared to a bulk active layer device. Finally, section V describes the results obtained with the most widely used MQW separate confinement heterostructure (SCH), comprising $In_{1-x}Ga_xAs$ (x=0.47) QW layers sandwiched between $In_{1-x}Ga_xAs_yP_{1-y}$ (x=0.30, y=0.63) barrier and waveguiding layers, and InP confining layers.

II. QW thickness determination

The emission wavelength in the QW layer corresponds to the transition energy between the first electron subband (E_{1e}) and the first heavy hole subband (E_{1h}). The energy levels E_{1e} and E_{1h} in the QW are calculated using the transcendental eigenvalue equation given by[9]:

$$tan(m_w E_{1e,h} L_z^2/2\hbar^2)^{1/2} =$$
$$= [m_w(\Delta E_{c,v} - E_{1e,h})/m_b E_{1e,h}]^{1/2},$$

where $m_w(m_b)$ is the effective mass of the carriers (electrons and holes) in the QW (barrier) layer, L, is the QW thickness, $\hbar$ is Planck's constant divided by 2π and $\Delta E_c(\Delta E_v)$ is the conduction (valence) band offset. The origin of the energies is at the bottom of the well for electrons and holes, respectively. We have considered the band offsets $\Delta E_c/\Delta E_g = 0.39$ and $\Delta E_v/\Delta E_g = 0.61$ [10], where ΔE_g is the band gap energy difference between the barrier and the QW layers, respectively. The emission wavelength is then given by the expression

$$\lambda_{em} = 1.2398/(E_g + E_{1e} + E_{1h}) ,$$

where λ_{em} is expressed in μm; E_g, E_{1e} and E_{1h} are expressed in eV, and E_g is the band gap energy of the QW material.

The band gap energy of $In_{1-x}Ga_xAs_yP_{1-y}$ lattice matched to InP was determined with the relation[11]:

$$E_g(eV) = 1.35 - 0.775y + 0.149y^2$$

The electron effective mass is given by[12]:

$$m_e/m_0 = 0.08 - 0.039y ,$$

where m_0 is the free electron mass. The heavy hole effective mass was obtained from a linear interpolation of the binaries values of GaAs, InP and InAs reported in Ref. [13], which results in the following expression:

$$m_{hh}/m_0 = 0.5x + 0.4(y - x) + 0.6(1 - y)$$

Note that the values of the energy gap and effective masses of InGaAs lattice matched to InP, are obtained using x=0.47 and y=1 in the formulas shown above.

The calculated results of the QW thickness for emission at $\lambda_{em} = 1.55\mu m$ as a function of the emission wavelength of the barrier layer is shown in Fig. 1. Note that the emission wavelength of the barrier increases as the barrier height of the QW decreases. Therefore, in order to maintain the emission wavelength of the QW structure fixed at 1.55μm, the QW thickness must also decrease. In this study we have considered two compositions of the barrier layers: InP and $In_{1-x}Ga_xAs_yP_{1-y}$ (x=0.30 and y=0.63) corresponding to emission wavelentghs of $0.92\mu m$ and $1.3\mu m$, respectively. According to Fig. 1, the InGaAs QW layer thicknesses necessary to obtain the 1.55μm emission with these barrier layers are 95Å and 70Å, respectively. These values are in agreement with reported QW thicknesses of 1.55μm lasers with corresponding similar MQW structures[3,7]. We have assumed in the following that the gain peak of the MQW laser device has the same wavelength as the ground state transition λ_{em} in the QW layers. The barrier thickness in the MQW structures were assumed to be 100Å.

III. MQW laser modelling

We have carried out a simple model of the dependence of the threshold current density (j_{th}) and the external quantum efficiency (η_{ext}) of the MQW laser as a function of the number of QWs (n,) and the length of the optical cavity (L). At threshold, the gain necessary to overcome the optical losses due to the light transmited through the end mirrors and the internal absorption of the cavity, is given by the equation[10]:

$$\Gamma g_{th} = \alpha_m + \alpha_{int} , \quad (1)$$

where Γ is the optical confinement factor of the active

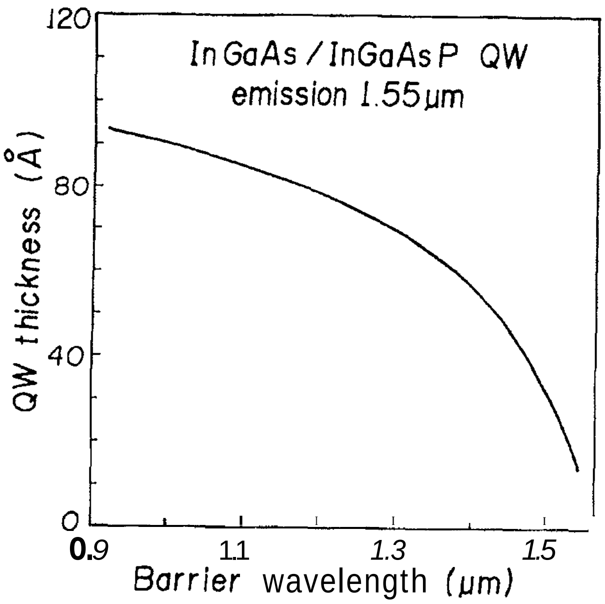

Figure 1: Plot of tlie QW thickness against tlie barrier emission rvavelength *in a lattice matched* InGaAs/InGaAsP QW emitting at 1.55μm.

layer. *a,* is the mirror loss absorption coefficient:

$$\alpha_m = (1/2L)\ln(1/R_1R_2) \ ,$$

where R_1 and R_2 are tlie end mirror reflectivities. $\alpha_{\rm int}$ is the absorption coefficient of the internal losses in the cavity:

$$\alpha_{int} = \alpha_s + (1-\Gamma)\alpha_c + \Gamma\alpha_c + \Gamma\alpha_{IVBA}$$

α_s is tlie scattering loss coefficient, α_C is the free carrier absorption loss and α_{IVBA} is the loss coefficient due to intervalence band absorption (IVBA) in the active layer. Following Fernier et al.[14], we have assumed α_{IVBA} to vary linearly with the carrier concentration:

$$\alpha_{IVBA} = K_0 n + \alpha_0 \ \ ,$$

where K_0 and α_0 are constants that depend oll the QW material and n is the carrier density.

In order to determine the carrier concentration at threshold n_{th} from Eq. (1), it is necessary to relate tlie gain peak g with n. Usually in QW lasers, this relation can be represented by a logarithmic expression. Following tlie procedure proposed by McIlroy et al.[15], tlie $g(n)$ expression can be accurately represented by:

$$g = g_0[\ln(n/n_0) + 1] \ , \tag{2}$$

where g_0 and n_0 are fitting parameters that depend on the QW structure. Introducing this expression into Eq. (1), we obtain thc following equation for the threshold carrier clensity:

$$n_{th} = n_0\beta\exp(K_0 n_{th}/g_0) \ \ , \tag{3}$$

where tlie coefficient ***3*** is given by:

$$\beta = \exp\{[\alpha_s+\alpha_c+(1/2L)\ln(1/R_1R_2)]/\Gamma g_0+\alpha_0/g_0-1\} \ .$$

Equation (3) cannot be solved in an analytical form, but it can be easily solved numerically with few iteration steps converging rapidly by assuming an initial value of $n_{th} = n_0$ on the rigth hand side. In some expressions of $g(n)$, a better fit is obtained without the g_0 term on the rigth hand side of Eq. (2). Then the equation of $n_{\rm th}$ remains the same as Eq. (3), but without the unity term in the exponential factor of the β coefficient. In the next sections we will describe the best fit employed for each MQW structure. In the calculations of n_{th} we have assumed the values reported in Ref. [14]: $R_1 = R_2 = 0.4$, *a,* $= 5$ cm^{-1}, $\alpha_s = 25$ cm^{-1} and α_0=45 cm^{-1}. The vulue of K_0 has been calculated in InGaAs/InP QWs[16], and was shown to be larger than in tlie bulk and to increase as tlie QW thickness decreases. From the knowledge of n_{th}, tlie threshold carrier density j_{th} can be easily calculated from[14,16]:

$$j_{th} = qn_zL_zB_{\rm eff}n_{th}^2 \ ,$$

wliere q is the electron charge and $B_{\rm eff}$ is the effective recombination coefficient. For the latter we have assumed the value $B_{\rm eff} = 1.4\times10^{-10}$ cm^3/s[14]. Note that $B_{\rm eff}n_{th}^2$ corresponds to the total carrier recombination rate, which includes non radiative mechanisms such as Auger recombination[14].

Finally, the determination of n_{th} allows us to obtain analytically the external quantum efficiency $\eta_{\rm ext}$ from the expression[10]:

$$1/\eta_{\rm ext} = (1/\eta_i)[1 + (\alpha_{\rm int}/\alpha_m)] \ ,$$

wliere η_i is the internal quantum efficiency that was assumed to be equal to unity.

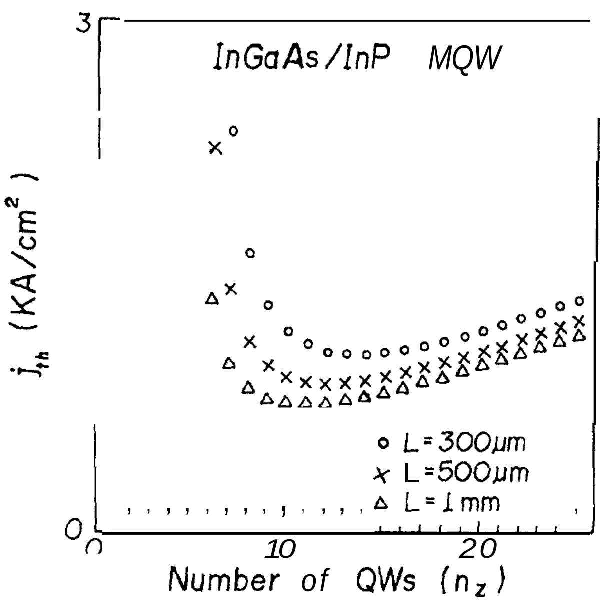

Figure 2: Threshold curreiit density as a function of the nuinber of wells in a MQW structure, calculated for different values of tlie cavity length.

IV. InGaAs/InP MQW structures

Tlie InGaAs/InP MQW structures consist of n_z InGaAs QW layers of thickness L_z=95Å sandwiched between InP barrier layers 100Å thiclr, which are confined with InP layers. The optical confinement factor Γ was calculated following the procedure described in Ref. [17], as the product of tlie confinement factor of the total MQW layers thickness with an average refractive index of the QW and barrier layers, by the ratio of the total QW thickness (n, L_z) to tlie total thickness of the MQW structure. The values of the refractive indexes of InGaAs and InP used to calculate Γ are 3.54 and 3.18[10], respectively. In order to determine n_{th} we have used the gain peak data as a function of the carrier density calculated by Asada et a~.['~which can be accurately represented by Eq. (2) with the fitting parameters: g_0 = 862.5cm^{-1} and $n_0 = 3.05 \times 10^{18}$cm^{-3}. For K_0 we have assumed tlie value reported in Ref. [16] for L, = 100Å which is $K_0 = 5.63 \times 10^{-17}$cm^2.

Figure 2 shows tlie dependence of the threshold current density j_{th} on the number of QWs for three values of the cavity length: L=300μm, 500μm and 1mm. One notices that for each curve there is a minimum value of j_{th}. Tlie value of Γ of a single QW layer is only 2 x 10^{-3}, and the gain necessary to compensate the optical loses in the laser cavity is very high when n, is small, and consequently j_{th} is also high. However, Γ increases as n_z also increases resulting in the lowering of j_{th} for mediuin values of n_z. But, as n_z increases further, the optical losses in the cavity also increase resulting in a slight increase of j_{th} for larger values of n_z. Thus, there is a minimum value of j_{th} as a function of n,. The minimum values of j_{th} for each value of L are the following: j_{th}=1.057KA/cm^2 and n_z=13 for L=300μm, j_{th}=0.883RA/cm^2 and n_z=12 for L=500μn, and j_{th}=0.758KA/cm^2 and n_z=11 for L=1mm. The results obtained for the shortest cavity laser are close to those reported in Ref. [16] for a similar MQW structure comprising QW and barrier layers 100Å thick. Note that j_{th} decreases as L decreases in Fig. 2, because of the exponential clepenclance on the inverse of L in the β coefficient in Eq. (3). This behaviour is due to a lower mirror loss as L increases, hence reducing the gain peak at threshold. If we now assume an index guided laser optical cavity of 2μm width and L=300μm, we obtain a threshold current ininimum about 6.3mA.

We have also calculated the external quantum efficiency $\eta_{\rm ext}$ for a cavity length L=300μm with n_z as a parameter. The values of $\eta_{\rm ext}$ obtained for n, varying from 10 to 18, range from 0.365 to 0.311, respectively. $\eta_{\rm ext}$ decreases as n, and L increase because the internal losses in the optical cavity also increase. However, when L becomes very small the mirror losses increase rapidly resulting in a β factor greater than one and consequently Eq. (3) does not converge, and therefore the gain peak cannot overcome the losses in the cavity. This point will be discussed further in the next section.

We can now compare these results with calculated values of the electro-optical characteristics of a device emitting at 1.55μm with a bulk active layer. For a device with an active layer 0.15μm thick corresponding to the minimum value of j_{th}, the value obtained with L = 400μm is $j_{th} \approx$1.77KA/cm^2 [14,16], and with L = 300μm one obtains $\eta_{\rm ext} \approx 0.295$[16]. Then, the threshold currerit minimuin of an index guided laser with an optical cavity of 2pm width and L = 300μm, is 10.6mA. The benefits of the MQW structure in the active layer of the laser device are therefore evident, in improving tlic electro-optical characteristics, due to the higher increase of the gain peak with the injected carrier density.

V. InGaAs/InGaAsP/InP MQW-SCHs

Tlie InGaAs/InGaAsP/InP SCH contains a. MQW structure with n_z InGaAs QW layers with L, = 70Å, sandwiched between InGaAsP barrier layers 100Å thick. On each side of tlie MQW structure there are separate confinement (SC) InGaAsP layers with an optimized thickness obtaincd as described below, which in turn are sandwiched between cladding layers of InP, hence completing the SCH. The composition of the InGaAsP material in the barrier and SC layers, respectively, corresponds to a. wavelength emission of $1.3\mu m$. We have calculated Γ in MQW-SCHs, by extending the procedure presented in Ref. [17] as follows. The total thickness of the optical waveguide includes the SC and the MQW layers, respectively. The refractive index of the InGaAs/InGaAsP MQW structure at the centre of tlie SCH is calculated with the average index described in Ref. [17]. Then the effective refractive intlex of the optical waveguide is calculated in tlie same manner, as tlie average index of the SC layers and the MQW structure. Γ is given as the product of the confinement factor in the optical waveguide thickness with its effective refractive index, by the ratio of tlie total QW thickness ($n_z L_z$) to the total thickness of tlie optical waveguide. The values of the refractive indexes used to calculate Γ are the same as above for InGaAs and InP, and for InGaAsP we have used the formula of Broberg and Lindgren[19].

The dependence of the confinement factor oii tlic SC layer thickness (L,,) of a single QW layer SCH with I,, = 70Å is presented in Fig. 3, for three values of the emission wavelength of the InGaAsP material. Note that L,, corresponds to the thickness of the SC layer on only one side of the QW. Γ increases rapidly with the SC layer thickness and with tlie lowering of

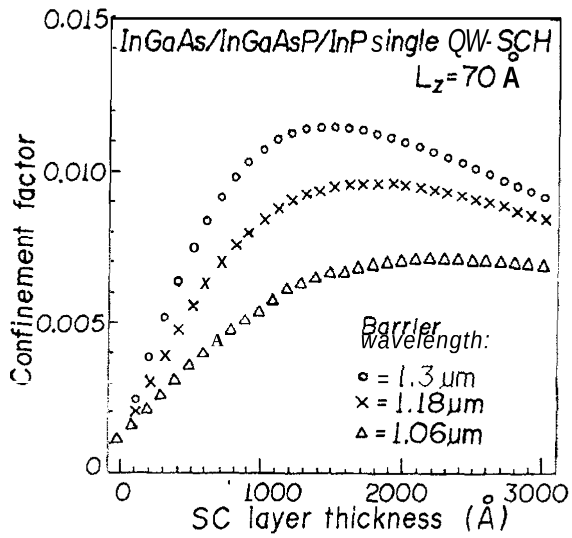

Figure 3: Optical confinement factor as a function of the SC layer thickness in a single QW-SCH, calciilated for different values of tlic InGaAsP (barrier) emission wavelength.

the band gap of tlie InGaAsP material. The optimized thickness for the $1.3\mu m$ SC layer is around 1500Å. Γ increases when the number of wells in the SCH increases, but the optimized thickness of the SC layer decreases for larger values of n_z. In fact, L_{sc} decreases linearly from about 1500Å to zero as n_z increases from 1 to 14, respectively. Tlie benefits of the SCH are therefore evident for increasing Γ and consequently reduce n, in tlic active layer, thus enabling tlie fabrication of a more simple MQW structure.

Tlie gain peak of an InGaAs/InGaAsP/InP QW-SCH emitting at $1.55\mu m$ with $1.3\mu m$ emission barrier and SC layers has been calculated by Rosenzweig et al.[8], and can be accurately represented by Eq. (2) without the g_0 term on the right hand side with the following fitting parameters: g_0=1687.7cm^{-1} and $n_0 = 1.354 \times 10^{18}$cm^{-3}. In this case: n_0 represents the carrier density required to reach transparency for population inversion. Tlie threshold carrier density is then determiiied with Eq. (3) without tlie unity term in the exponential factor of β, as described in section III. For the IVBA constant K_0, we have used the value reported in Ref. [16] for L, = 50Å which corresponds to $K_0 = 9.8 \times 10^{-17}$cm^2, somewhat larger than before due to tlie smaller QW thickness. Figure 4 shows the dependence of j_{th}, on 12, for three values of L : $300\mu m$, $500\mu m$

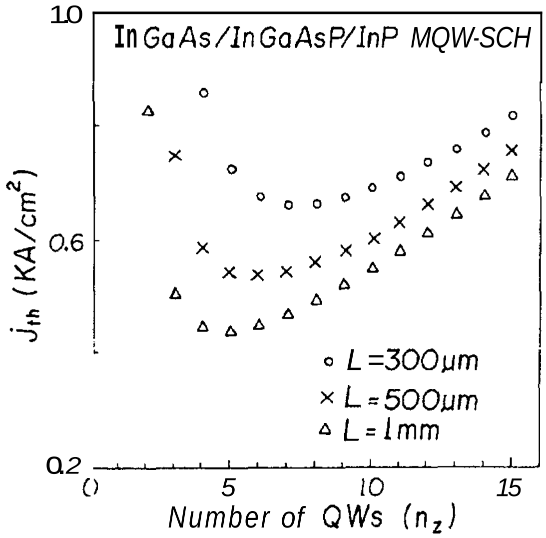

Figure 4: Threshold current density as a function of the number of wells in a MQW-SCH, calculated for different values of the cavity length.

and 1mm. One notices that a lower j_{th} is obtained in conjunction with a smaller n_z compared to Fig. 2. The reason is the increase of Γ in the SCH due the InGaAsP SC layer. The minimum values obtained for the threshold current density are as follows: j_{th}=0.66KA/cm^2 and n_z=7 for L = 300μm, j_{th}=0.535KA/cm^2 and n_z=6 for L = 500μm, and j_{th}=0.44KA/cm^2 and n_z = 5 for L, = 1mm. The optimized SC layer thickness decreases from 1000Å to about 750Å, as n_z increases from 5 to 7, respectively. One also notices a decrease of j_{th} as L increases, for the same reasons described for the InGaAs/InP MQW laser structure in the previous section. If we assume an index guided optical laser cavity of 2μm width and L = 300μm, we obtain a threshold current min mum about 4mA. The external quantum efficiencies calculated for MQW-SCHs with L = 300μm range from η_{ext}=0.376 to 0.36 for n_z=5 to 7, respectively. These values are higher than those obtained for the same cavity length in an InGaAs/InP MQW laser, because of the larger increase of the gain peak with carrier density in the MQW-SCH.

We have also considered for the MQW-SCH a more realistic value of the carrier density at transparency extracted from experimental data reported in Ref. [8], which gives n_0 = 1.72 x 10^{18}cm^{-3}. This higher value is attributed to additional losses involving a high den-

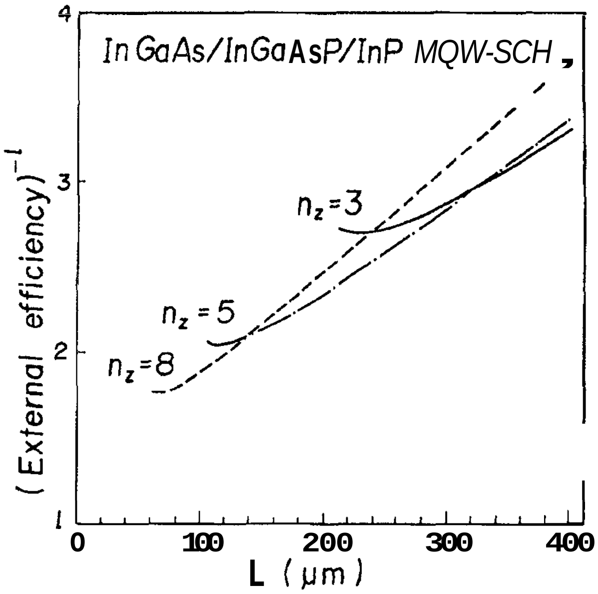

Figure 5: Inverse of the external quantum efficiency as a function of the cavity length in MQW-SCH, calculated for different values of the number of wells.

sity of electronic states at the interfaces in the MQW layers, which have to be saturated before gain can be obtained. Using this larger value of n_0, the calculated values of j_{th} are somewhat shifted to higher values relative to Fig. 4, but with little modification of n,. In this case, the minimum j_{th} values obtained are the following: j_{th}=1.143KA/cm^2 and n_z=8 for L = 300μm, j_{th}=0.928KA/cm^2 and n_z=6 for L = 500μm, and j_{th}=0.762KA/cm^2 and n_z=5 for L = 1mm. Note that the j_{th} values are close to those predicted for the InGaAs/InP MQW laser. The threshold current minimum of the index guided cavity of 2pm width and L = 300μm, is about 6.8mA. However, η_{ext} is lower than the previous case, the calculated values obtained with L = 300μm vary from η_{ext}=0.35 to 0.323 for n_z=5 to 8, respectively; but they are still higher than those calculated for a bulk active layer device emitting at the same wavelength.

The dependence of the inverse of η_{ext} on the cavity length is shown in Fig. 5, with n_z as a varying parameter. In this calculation, we have assumed the experimental value of the carrier density at transparency n_0 = 1.72 × 10^{18}cm^{-3}. As expected, η_{ext} decreases as L and n_z increases. However, one notices that for short cavity lasers, as L decreases η_{ext} saturates and then decreases, because the mirror losses become important. This effect is more pronounced for a lower n_z due to the smaller optical confinement factor. Therefore, tlie maximum value of η_{ext} decreases as n_z also decreases in conjunction with an increasing value of L. In very sliort cavity lasers, the gain does not overcome the losses of tlie optical cavity and Eq. (3) has no possihle solution, hence tlie device cannot lase. These results are in agreement with reported data on short cavity QW lasers of GaAs/GaAlAs, mhere an increase of tlie threshold current was observed for L $\leq 300\mu$m [20].

VI. Conclusion

In conclusion, we have presented a theoretical model for the dependence of the electro-optical characteristics of 1.55μm MQW lasers on geoinetrical parameters of the optical cavity. We have analyzed two lattice matched MQW structures: InGaAs/InP and InGaAs/InGaAsP/InP SCHs comprising 1.3μm emitting SC layers. We have demonstrated the influence of the number of QWs and tlie cavity length on the threshold ciirrent density and tlie external quantum efficiency, taking into account tlie intervalence band absorption losses in the QW layers. The threshold current density j_{th} has a minimum value as a function of n_z, mhich decreases as L increases. The external quantum efficiency η_{ext} increases as n_z and L decreases. The minimum values of j_{th} and corresponding values of n_z are lowered in InGaAs/InGaAsP/InP MQW-SCHs, due to the enhancement of the optical confinement factor in tlie SCH. The results obtained in both MQW structures present improved electro-optical characteristics, compared to a device with a bulk active layer emitting at the same wavelength.

References

1. M. G. Burt, Electron. Lett. **19**, *210* (1983).
2. T. P. Lee, Proceedings of the IEEE Edited by Institute of Electrical and Electronics Engineers (IEEE) 79, 253 (1991).
3. W. T. Tsang, IEEE J. Quantum Electron. **QE-23**, 936 (1987).
4. U. Koren, B. I. Miller, Y. KSu, T. L. Kock and J. E. Bowers, Appl. Phys. Lett. 51, 1744 (1987).
5. T. Tanbun-Ek, R. A. Logan, H. Temkin, K. Berthold, A. F. J. Levi and N. G. Chu, Appl. Phys. Lett. 55, 2283 (1989).
6. A. Perales, L. Goldstein, A. Accard, B. Fernier, F. Leblond and C. Gourclain, Electron. Lett. 26, 236 (1990).
7. A. Ougazzaden, J. D. Ganiere, Y. Gao, E. V. K. Rao, B. Sermage, C. Kazmierski and A. Mircea, J. Cryst. Growth 107, 761 (1.991).
8. M. Rosenzweig, M. Mohrle, H. Duser and H. Venghaus, IEEE J. Quantum Electron. QE-27, 1804 (1991).
9. G. Bastard and J. A. Brum, IEEE J. Quantum Electron. QE-22, 1625 (1986).
10. G. P. Agrawal and N. K. Dutta, Long *Wavelength Semiconductor Lasers*, Edited by S. Mitra (Van Nostrand, New York, 1986).
11. T. P. Pearsall, *GaInAsP Alloy Semiconductors*, (Wiley, New York, 1982).
12. R. J. Nicholas, A. M. Davidson, S. J. Sessions and R. A. Stradling, IEEE J. Quantum Electron. **QE-**17, 145 (1981).
13. M. Schur, *Physics of Semiconductor Devices*, Ed. N. Holonyak Jr. (Prentice Hall, London, 1990).
14. B. Fernier, P. Brosson, J. P. Jicquel and J. Benoit, IEE Proceeclings, Edited by Institution of Electrical Engineers (IEE), **134,** PtJ, 27 (1987).
15. P. W. A McIlroy, A. Kurobe and Y. Uematsu, IEEE J. Quantum Electron. QE-21, 1958 (1985).
16. M. Asada, A. Kameyama and Y. Suematsu, IEEE J. Quantum Electron. QE-20, 745 (1984).
17. W. Streifer, D. R. Scifres and D. Burnham, Appl. Optics 18, 3547 (1979).
18. M. T. Furtado, unpublished results.
19. B. Broberg and S. Lindgren, **3.** Appl. Phys. 55, 3376 (1984).
20. A. R. Reisenger, P. S. Zory and R. G. Waters, IEEE J. Quantum Electron. QE-23, 993 (1987).